



Host Cell Metabolism Contributes to Delayed-Death Kinetics of Apicoplast Inhibitors in *Toxoplasma gondii*

Katherine Amberg-Johnson,^a Ellen Yeh^{a,b,c,d}

^aDepartment of Microbiology and Immunology, Stanford University, Stanford, California, USA

^bDepartment of Biochemistry, Stanford University, Stanford, California, USA

^cDepartment of Pathology, Stanford University, Stanford, California, USA

^dChan Zuckerberg Biohub, San Francisco, California, USA

ABSTRACT *Toxoplasma gondii* and related human parasites contain an essential plastid organelle called the apicoplast. Clinically used antibiotics and other inhibitors that disrupt apicoplast biogenesis cause a mysterious “delayed-death” phenotype in which parasite growth is unaffected during the first lytic cycle of inhibitor treatment but is severely inhibited in the second lytic cycle even after drug removal. Critical to understanding the complex downstream cellular effects of these drug classes are the timing of apicoplast loss during inhibitor treatment and how it relates to this peculiar growth phenotype. Here we show that, upon treatment with diverse classes of apicoplast inhibitors, newly replicated *T. gondii* parasites in the first lytic cycle initially form apicoplasts with defects in protein import or genome replication and eventually fail to inherit the apicoplast altogether. Despite the accumulation of parasites with defective or missing apicoplasts, growth is unaffected during the first lytic cycle, as previously observed. Strikingly, concomitant inhibition of host cell isoprenoid biosynthesis results in growth inhibition in the first lytic cycle and unmasks the apicoplast defects. These results suggest that defects in and even the complete loss of the apicoplast in *T. gondii* are partially rescued by scavenging of host cell metabolites, leading to death that is delayed. Our findings uncover host cell interactions that can alleviate apicoplast inhibition and highlight key differences in delayed-death inhibitors between *T. gondii* and *Plasmodium falciparum*.

KEYWORDS *Plasmodium falciparum*, *Toxoplasma gondii*, antimalarial agents, antiparasitic agents, apicoplast, host-parasite relationship

The Apicomplexa phylum contains human and animal parasites, including *Toxoplasma gondii*, which causes opportunistic infections, and *Plasmodium* spp., which cause malaria. These parasites contain an essential plastid organelle called the apicoplast that is derived from secondary endosymbiosis of a red alga (1–3). While the apicoplast is no longer photosynthetic, it houses essential pathways for biosynthesis of fatty acids, heme, iron-sulfur clusters, and isoprenoid precursors (4–6). Apicoplast ribosome inhibitors, such as clindamycin and doxycycline, are used clinically for treatment of acute toxoplasmosis and malaria chemoprophylaxis, respectively (7, 8). In both *T. gondii* tachyzoites and blood-stage *P. falciparum*, these inhibitors cause a peculiar “delayed-death” phenotype *in vitro*: treatment with inhibitors during the first lytic cycle has no effect on parasite replication, egress of daughter parasites from the first host cell, or reinfection of new host cells. However, parasites subsequently fail to replicate in the second lytic cycle, even if the inhibitor is removed (9–11). In addition to structurally diverse antibiotics targeting the prokaryotic ribosome, inhibitors of DNA gyrase (ciprofloxacin) and the apicoplast membrane metalloprotease FtsH1 (actinonin) also cause delayed death in *T. gondii*, indicating that drug properties do not account for the

Citation Amberg-Johnson K, Yeh E. 2019. Host cell metabolism contributes to delayed-death kinetics of apicoplast inhibitors in *Toxoplasma gondii*. *Antimicrob Agents Chemother* 63:e01646-18. <https://doi.org/10.1128/AAC.01646-18>.

Copyright © 2019 Amberg-Johnson and Yeh. This is an open-access article distributed under the terms of the [Creative Commons Attribution 4.0 International license](https://creativecommons.org/licenses/by/4.0/).

Address correspondence to Ellen Yeh, ellenyeh@stanford.edu.

Received 5 August 2018

Returned for modification 2 September 2018

Accepted 8 November 2018

Accepted manuscript posted online 19 November 2018

Published 29 January 2019

delayed growth inhibition and that delayed death is likely a result of complex downstream cellular effects of apicoplast inhibitors (9, 10, 12, 13).

Each of these apicoplast inhibitors causes defects in the biogenesis of the apicoplast—its growth, division, and inheritance—leading to the formation of *T. gondii* parasites that are missing the apicoplast entirely (10, 12, 13). It is therefore surprising that these drug-treated parasites replicate to wild-type levels in the first lytic cycle during inhibitor treatment, as defects in or loss of the apicoplast should render parasites unable to produce essential apicoplast-derived metabolites (14). How parasites are able to compensate for this loss during the first lytic cycle remains poorly understood. Of note, growth kinetics resembling delayed death have also been observed for inhibitors that block apicoplast metabolic function and genetic disruption of proteins required for apicoplast biogenesis or metabolism, suggesting that inhibiting the production of essential apicoplast metabolites may be the common perturbation leading to delayed death in *T. gondii* (4, 5, 15–17).

A number of models have been proposed to explain how apicoplast defects lead to delayed death. One model proposes that apicoplast metabolites are required only for the successful establishment of a parasitophorous vacuole (PV) but are dispensable during intravacuolar replication (9). Another model proposes that growth of parasites with defective apicoplasts during the first lytic cycle is supported by sister parasites with functioning apicoplasts in the same vacuole (18). These models, however, are inconsistent with data from experiments in which clindamycin-treated parasites were manually released from the host cell prior to completion of the first lytic cycle, separated from sister parasites, and allowed to establish a new infection. These drug-treated, prematurely lysed parasites were able to establish a new PV and replicate albeit at reduced rates that depended on the duration of drug treatment and number of replications in the previous vacuole (9). These parasites also eventually fail to replicate in the third or, with continued manual release, later lytic cycles (9), suggesting that the “delay” in growth inhibition is not strictly tied to lytic cycles. Thus, neither of the proposed models is sufficient to explain the delayed-death phenotype.

Several key questions remain. First, what is the timing of apicoplast biogenesis defects and loss upon treatment with apicoplast inhibitors? Apicoplast loss is an important downstream cellular consequence of these inhibitors but has not been quantified during a full lytic cycle. Second, do apicoplast inhibitors with distinct molecular targets lead to different rates of apicoplast loss? While the literature suggests similar phenotypes between diverse classes of apicoplast inhibitors, this has yet to be confirmed with a side-by-side comparison. Third, what is the role of the host cell in delayed death? We hypothesize that since *T. gondii* replicates in a metabolically active host cell, host metabolites may compensate for apicoplast inhibition. Fourth, how do the downstream cellular effects of apicoplast inhibition differ between *T. gondii* and *Plasmodium falciparum*? Their distinct replication cycles, differences in their host cell metabolic activity, and the overlapping but distinct inhibitor classes that cause delayed death in these parasites suggest different mechanisms underlie the seemingly similar delayed growth kinetics.

To address these questions, we validated an apicoplast marker to monitor apicoplast biogenesis defects and loss and show that multiple classes of apicoplast inhibitors cause a gradual accumulation of parasites with disrupted or missing apicoplasts. Interestingly, the delayed-death growth kinetics caused by these apicoplast inhibitors is modulated by an inhibitor of host cell isoprenoid biosynthesis. These results clarify the complex downstream cellular effects of apicoplast inhibition on *T. gondii* and their similarities to and differences from those on *P. falciparum*.

RESULTS

Apicoplast inhibitors cause reduced or absent FNR-RFP, an apicoplast marker.

We selected three inhibitors that are well documented to cause delayed death in *T. gondii* and have strong evidence for their target in the apicoplast: actinonin (membrane metalloprotease FtsH1), clindamycin (ribosome), and ciprofloxacin (DNA gyrase) (5, 10,

12, 13, 19). The apicoplast had been previously observed by microscopy of *T. gondii* RH parasites expressing an apicoplast-targeted ferredoxin NADP⁺ reductase fused to red fluorescence protein (FNR-RFP) (12, 17, 20–23). In experiments with these parasites, treatment with apicoplast inhibitors leads to vacuoles with some parasites missing FNR-RFP fluorescence (10, 12, 17). While those studies suggested that the inhibitors lead to disruption of apicoplast biogenesis, it was unclear exactly how FNR-RFP fluorescence corresponded to apicoplast presence. Furthermore, since those studies used microscopy, they could count apicoplasts only in vacuoles containing <8 parasites, corresponding to no more than 3 replications out of >6 total replications during the lytic cycle (10, 12, 17). To clarify those initial observations, we sought to develop a quantitative method to monitor apicoplast loss through a full lytic cycle. Because microscopy of large vacuoles with 8 or more parasites is difficult, we used flow cytometry to count and quantify the FNR-RFP fluorescence of individual extracellular parasites after host cell egress.

We compared FNR-RFP fluorescence with the presence of the apicoplast genome, a known apicoplast marker. Briefly, parasites were treated with actinonin, clindamycin, or ciprofloxacin for a single lytic cycle. After natural egress from the first lytic cycle, egressed parasites were collected, and their FNR-RFP fluorescence was quantified by flow cytometry (Fig. 1A and B). While untreated parasites retained high levels of FNR-RFP fluorescence, treatment with each apicoplast inhibitor generated two populations of parasites: one devoid of FNR-RFP fluorescence [FNR-RFP⁻] and one in which FNR-RFP was detectable but with a mean fluorescence intensity 25% to 75% lower than that of the untreated population [FNR-RFP^{reduced}]. We sorted these two populations and quantified their apicoplast/nuclear genome ratios by quantitative PCR (qPCR) (Fig. 1C; see also Table S1 in the supplemental material). The apicoplast genome was present at reduced levels compared to those of untreated parasites but still detectable in FNR-RFP^{reduced} parasites. In contrast, the apicoplast genome level was below the detection limit in FNR-RFP⁻ parasites, consistent with the loss of the apicoplast in FNR-RFP⁻ parasites. These results validate the use of FNR-RFP fluorescence as a marker for apicoplast presence. It also suggests that while FNR-RFP^{reduced} cells still contain the apicoplast, the apicoplast is defective given the reduced levels of FNR-RFP fluorescence, the lower apicoplast genome copy numbers, and the failure of both populations to grow in the next lytic cycle (10, 12, 13).

Apicoplast loss occurs gradually during the first lytic cycle. During the *T. gondii* lytic cycle, a single parasite undergoes >6 synchronous rounds of binary division, forming >64 daughter parasites within a vacuole in the host cell (24). Apicoplast growth, division, and inheritance are coordinated with parasite replication, leading to exactly one apicoplast per parasite (25). Because parasites grow to wild-type levels during the first lytic cycle during treatment, we were surprised to find that the large majority of parasites had either disrupted or undetectable apicoplasts at this time point (Fig. 1A to C). We therefore further characterized the timing of apicoplast disruption during the first lytic cycle.

T. gondii parasites were treated with apicoplast biogenesis inhibitors, and parasites were harvested after 6, 12, 24, 36, or 48 h of treatment (Fig. 2A). At each time point, we manually released parasites from host cells and assessed apicoplast status based on (i) apicoplast genome levels, (ii) the import of endogenous nucleus-encoded apicoplast proteins (26), (iii) the mean FNR-RFP fluorescence intensity of the population retaining a detectable FNR-RFP signal, and (iv) the percentage of cells containing detectable FNR-RFP (NB: only apicoplast genome levels were assessed at the 6-h time point).

In the first 12 h of the lytic cycle, *T. gondii* parasites invade host cells, establish a new PV, and divide once or twice. During this time, the only apicoplast defect observed is a slight reduction in the level of the apicoplast genome for parasites treated with actinonin and ciprofloxacin (Fig. 2B and Table S1). After 24 h, parasites have completed 3 to 4 divisions, and reductions in levels of the apicoplast genome are detected for all apicoplast inhibitors (Fig. 2B). Also at this time point, other apicoplast defects start to

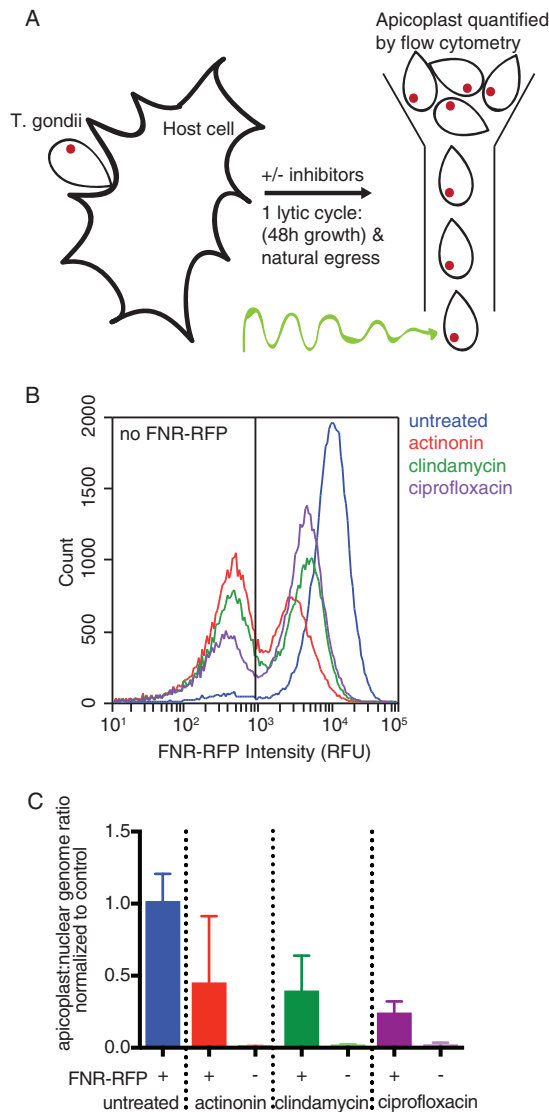


FIG 1 Apicoplast inhibition causes reduced or absent FNR-RFP, which is correlated with apicoplast genome levels. (A) Schematic of the experimental procedure. *T. gondii* is allowed to infect host cells for a single lytic cycle in the presence or absence of apicoplast inhibitors. The resulting parasites are collected and analyzed by flow cytometry. (B) Representative histogram of FNR-RFP fluorescence intensity of parasites after a single lytic cycle of growth in the presence or absence of apicoplast inhibitors. The nonfluorescent gate was drawn based on parasites that did not express FNR-RFP or any other fluorescent marker. RFU, relative fluorescence units. (C) Apicoplast/nuclear genome ratios of sorted parasites after a single lytic cycle of growth in the presence or absence of apicoplast inhibitors. Gates to sort FNR-RFP⁺ or FNR-RFP⁻ parasites were drawn based on parasites that did not express FNR-RFP. Data are representative of results from two biological replicates performed in technical triplicate. Error bars represent the standard errors of the means (SEM).

appear. We observed that drug-treated parasites lack processing of the apicoplast protein Cpn60 and instead accumulate the full-length protein (Fig. 2C), indicating a defect in apicoplast protein import. The FNR-RFP fluorescence of parasites expressing measurable FNR-RFP starts to dim for parasites treated with actinonin and clindamycin (Fig. 2D and Table S1). Finally, FNR-RFP⁻ parasites start to emerge in samples treated with actinonin (Fig. 2E and Table S1). These defects continue to accumulate for all drug-treated parasites. By 48 h, *T. gondii* has completed 6 to 8 divisions and egressed from the host cell. At this time point, the apicoplast genome levels are reduced to 8% to 22% (Fig. 2B and Table S1), the proportion of (full-length [FL]) *T. gondii* Cpn60 (*TgCpn60*) has increased (Fig. 2C), the mean level of FNR-RFP fluorescence in the

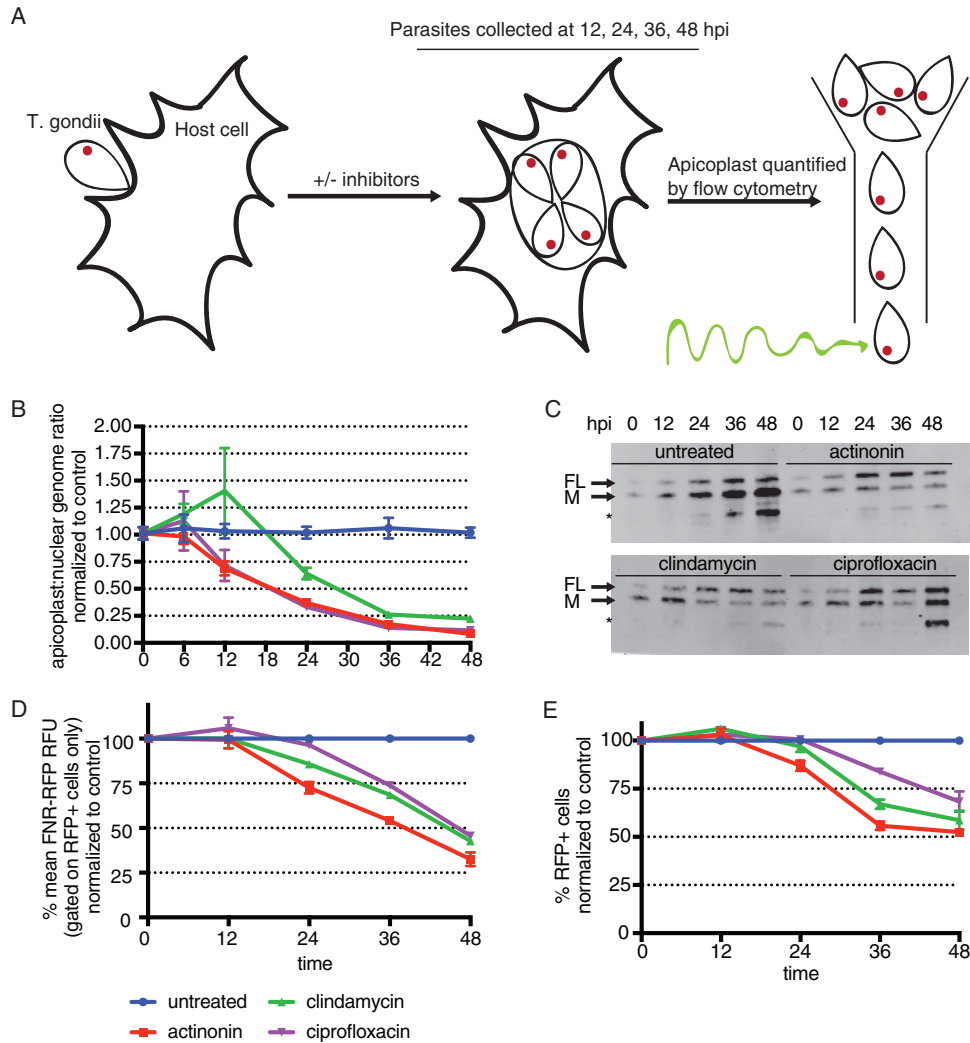


FIG 2 Apicoplast loss occurs gradually over the first lytic cycle of treatment. (A) Schematic of the experimental procedure. *T. gondii* parasites are allowed to infect host cells and grow in the presence or absence of apicoplast inhibitors. At 6, 12, 24, 36, or 48 h, parasites are manually released from host cells. Because host cell lysis occurs between 36 and 48 h, parasites analyzed at these time points may reflect growth in the second lytic cycle. hpi, hours postinfection. (B) Apicoplast/nuclear genome ratios at all time points. Data are representative of results from two biological replicates performed in technical triplicate. Error bars represent the SEM. (C) Western blotting of *TgCpn60* from 12 to 48 h. FL indicates the full-length protein prior to transit peptide cleavage. M indicates the mature protein after import into the apicoplast and transit peptide cleavage. The asterisk designates a probable cross-reacting signal (26). Data are representative of results from two biological replicates. (D) Mean FNR-RFP fluorescence of parasites with detectable FNR-RFP fluorescence, normalized to values for control untreated parasites, from 12 to 48 h. Data are representative of results from two biological replicates. Error bars represent the SEM. (E) Percentages of cells with detectable FNR-RFP fluorescence, normalized to values for control untreated parasites, from 12 to 48 h. Data are representative of results from two biological replicates. Error bars represent the SEM.

FNR-RFP^{reduced} population is 25% to 50%, and 25% to 50% of parasites lose FNR-RFP fluorescence altogether [FNR-RFP⁻] compared to untreated control parasites. Overall, we observe that *T. gondii* parasites treated with apicoplast inhibitors exhibit apicoplast biogenesis defects by as early as the second round of parasite replication and that the severity of these defects worsens throughout the first lytic cycle of treatment, despite normal growth.

Host isoprenoids are necessary for growth in the first lytic cycle upon treatment with apicoplast inhibitors. Because *T. gondii* parasites treated with apicoplast inhibitors accumulate apicoplast biogenesis defects and lose their apicoplast long before growth inhibition is observed (Fig. 2D and E), we sought to determine whether the scavenging of host cell metabolites can compensate for the loss of one or more

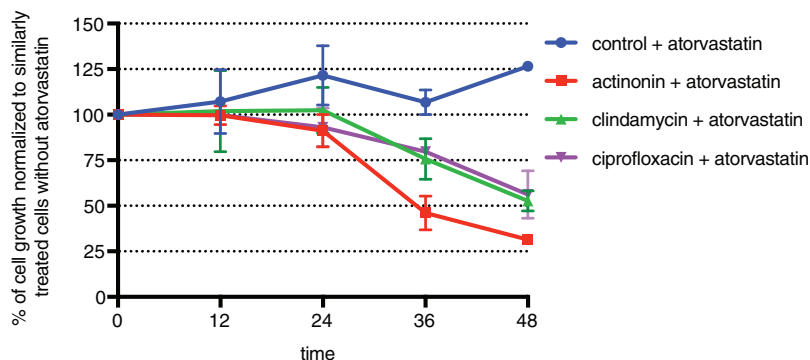


FIG 3 Inhibition of host isoprenoid biosynthesis with atorvastatin results in growth kinetics that deviate from delayed death. Parasite growth was quantified by flow cytometry of *T. gondii* parasites manually released from host cells at each time point after treatment with atorvastatin and in the presence or absence of apicoplast drugs. Growth is normalized to that of parasites treated with the same apicoplast inhibitor but in the absence of atorvastatin at each time point. Data are representative of results from two biological replicates. Error bars represent the SEM. Because host cell lysis occurs between 36 and 48 h, parasites analyzed at these time points may reflect growth in the second lytic cycle.

apicoplast metabolic functions. Isoprenoid biosynthesis is an essential function of the apicoplast (5, 6), and scavenging of host cell isoprenoids by *T. gondii* was shown previously (27). Therefore, parasites were cotreated with apicoplast inhibitors and atorvastatin, a specific inhibitor of host cell isoprenoid biosynthesis. As seen previously, treatment with 13 μM atorvastatin alone did not affect parasite growth, suggesting that in the presence of an intact apicoplast host cell, isoprenoid biosynthesis is not essential (Fig. 3; see also Fig. S1 in the supplemental material) (27). However, unlike atorvastatin or apicoplast inhibitors alone, the combination of atorvastatin with actinonin, clindamycin, or ciprofloxacin caused parasite growth inhibition within the first lytic cycle (Fig. 3, Fig. S1, and Table S1). Instead of growing to wild-type levels during a full 48-h lytic cycle, growth defects are detectable as early as 24 h after treatment (Fig. 3, Fig. S1, and Table S1). After 48 h, parasites cotreated with atorvastatin and apicoplast inhibitors show 30% to 50% growth compared to parasites treated with apicoplast inhibitors only (Fig. 3 and Table S1). The MICs of apicoplast inhibitors for growth inhibition were similar in the presence and absence of atorvastatin, indicating that atorvastatin's potential effect on host cell permeability did not result in off-target effects (MIC of 20 μM for actinonin with or without atorvastatin, MIC of 4 nM for clindamycin with or without atorvastatin, and MIC of 12.5 μM for ciprofloxacin with or without atorvastatin). Rather, the altered kinetics of growth inhibition suggest that with the loss of apicoplast function, parasites either require host isoprenoid biosynthesis after 24 h or deplete host isoprenoid reservoirs after 24 h. We favor the former model since pretreatment of host cells with atorvastatin for 24 h prior to infection with *T. gondii* showed similar results (Fig. S2 and Table S1).

DISCUSSION

Our findings suggest the following model for the downstream cellular effects of apicoplast inhibitors on *T. gondii*. First, several classes of apicoplast inhibitors cause an accumulation of apicoplast biogenesis defects and eventual apicoplast loss. We detect these defects beginning as early as the second round of parasite replication in the first lytic cycle, preceding growth defects in the second lytic cycle.

Second, apicoplast biogenesis defects disrupt apicoplast biosynthetic functions important for both intravacuolar growth and, likely, the establishment of infection in new host cells. This model predicts that direct inhibition of apicoplast biosynthetic pathways, without disrupting apicoplast biogenesis, will also cause delayed death, consistent with previous observations in the literature (4, 16).

Third, scavenging of host cell metabolites in the first lytic cycle can substitute for metabolites normally biosynthesized in the apicoplast. We specifically tested the

scavenging of host cell isoprenoids, which was required 24 h into the first lytic cycle. Host fatty acids and heme may also compensate for the loss of these apicoplast biosynthetic functions, although we were unable to directly test these pathways given the lack of specific inhibitors. Overall, we propose that host cell metabolites support the growth of *T. gondii* during the first lytic cycle of apicoplast inhibition. Our results add to a growing body of work indicating that access to host metabolites regulates the essentiality of parasite metabolic pathways and the organelles that provide them (27–31).

Finally, host cell metabolites cannot compensate for the apicoplast indefinitely, since parasites treated with apicoplast inhibitors ultimately fail to replicate in later lytic cycles. It is possible that metabolites sourced from the apicoplast are required at the beginning of the lytic cycle for PV formation and host cell remodeling. If this is true, then drug-treated parasites prematurely lysed from host cells may continue to grow in subsequent lytic cycles because the apicoplast is still partially functional at these early time points. Alternatively, a combination of host cell scavenging and accrued apicoplast metabolites may be sufficient during the first lytic cycle but ultimately become depleted in subsequent lytic cycles. More experiments are required to differentiate between these scenarios and ultimately reveal the essential products of the *T. gondii* apicoplast.

These downstream cellular effects of apicoplast biogenesis inhibitors on *T. gondii* differ from the known effects on *P. falciparum* in significant ways. First, we show that *T. gondii* parasites lacking apicoplasts accumulate over multiple parasite replications during the first lytic cycle. In contrast, blood-stage *P. falciparum* undergoes only a single round of parasite replication during each host lytic cycle, and apicoplast biogenesis is largely unaffected by treatment with apicoplast translation inhibitors during the first lytic cycle (a small reduction in apicoplast genome copy numbers is sometimes observed) (11, 32). Second, we show that *T. gondii* parasites lacking apicoplasts are viable during the first lytic cycle, and apicoplast loss and parasite growth inhibition are temporally separated. In contrast, *P. falciparum* growth inhibition occurs concurrently with apicoplast biogenesis defects in the second lytic cycle, most likely because apicoplast loss cannot be overcome by scavenging of host cell metabolites (6, 11). We suspect that this is due to the different metabolic activities of their respective host cells: while *P. falciparum* grows in relatively inert red blood cells, *T. gondii* makes its home in metabolically active host cells. Third, while all known apicoplast inhibitors cause delayed death in *T. gondii*, only the subset of apicoplast inhibitors that disrupt apicoplast genome expression cause delayed death in *P. falciparum* (12). The common defect leading to delayed death in *T. gondii* appears to be the loss of apicoplast metabolic function, while the common defect in *P. falciparum* delayed death is the loss of apicoplast genome expression. While it is possible that different molecular targets account for these different inhibitor phenotypes, all apicoplast inhibitors used in this study have strong evidence for the same target in both organisms (10, 12, 13, 32). Instead, these different downstream cellular effects of apicoplast inhibitors likely reflect the different biology of the parasites and their dependence on apicoplast metabolic function.

MATERIALS AND METHODS

Chemicals. Actinonin was purchased from Sigma-Aldrich, and 25 mM aliquots were prepared in ethanol. Clindamycin was purchased from Sigma-Aldrich, and 5 μ M aliquots were prepared in water. Ciprofloxacin was purchased from Sigma-Aldrich, and 50 μ M aliquots were prepared in water. Atorvastatin was a gift from the Smolke laboratory at Stanford, and 50 μ M aliquots were prepared in dimethyl sulfoxide (DMSO).

***Toxoplasma gondii* culture.** *T. gondii* RH FNR-RFP (25) was a gift from Boris Striepen (University of Pennsylvania). Parasites were maintained by passage through confluent monolayers of human foreskin fibroblast (HFF) host cells. HFFs were cultured in Dulbecco's modified Eagle's medium (DMEM) (Invitrogen) supplemented with 10% fetal bovine serum (FBS) (Fetal Plex animal serum; Gemini, West Sacramento, CA), 2 mM L-glutamine (Gemini), and 100 μ g penicillin and 100 μ g streptomycin per ml (Gibco Life Technologies) and maintained at 37°C with 5% CO₂. Parasites were harvested for assays by syringe lysis of infected HFF monolayers.

Growth inhibition assays. A total of 1.5 million extracellular tachyzoites were counted by flow cytometry and allowed to infect confluent HFFs in T25 flasks. This amount of parasites was chosen because it leads to lysis of the host monolayer after a 48-h lytic cycle. Infected cells were then incubated with either no apicoplast inhibitor, 40 μM actinonin, 100 nM clindamycin, or 25 μM ciprofloxacin. When included, 13 μM atorvastatin was used. At designated time points during the first lytic cycle, parasites were released from HFFs using syringe lysis and either counted by flow cytometry (BD Accuri C6 sampler) or collected for qPCR (7900HT; Applied Biosystems) or immunoblotting. All time course experiments were repeated with at least 2 biological replicates.

Flow cytometry and sorting. Fluorescence-activated cell sorting (Sony) was performed on FNR-RFP parasites grown for a full lytic cycle with either no drug, 40 μM actinonin, 100 nM clindamycin, or 25 μM ciprofloxacin. Untagged parasites were used for gating on FNR-RFP⁻ cells. One million cells were sorted from each population and frozen at -80°C for subsequent analysis.

Flow cytometry (BD Accuri C6 sampler) was performed to count parasites and quantify FNR-RFP fluorescence. Untagged parasites were used for gating on FNR-RFP⁻ cells. At each time point, syringe-lysed cells were washed and resuspended in phosphate-buffered saline (PBS), and 10- μl fixed volumes were quantified. Samples were always resuspended in PBS directly prior to measurement in the flow cytometer.

Quantitative real-time PCR. At each time point, syringe-lysed parasites (1 ml of culture, representing one-fourth of the total sample) were collected, spun down, and frozen prior to analysis. DNA was purified using a DNeasy blood and tissue kit (Qiagen, Germany). Primers were designed to target genes found on the apicoplast or nuclear genome, *tufA* (apicoplast) (5'-TGGAGCCGCACAAATGGAT-3'/5'-CTT AGTTTGTGGCATTGGCCC-3') and actin (nuclear) (5'-GCGCGACATCAAGGAGAAGC-3'/5'-CATCGGGCAATT CATAGGAC-3') (33). Reaction mixtures contained template DNA, 0.15 μM each primer, and 1 \times SYBR green I master mix (Roche). qPCR reactions were performed at 56 $^{\circ}\text{C}$ for primer annealing and at 65 $^{\circ}\text{C}$ for template extension for 35 cycles on an Applied Biosystems 7900HT system. Relative quantification of target genes was performed as described previously (34). For each time point, the apicoplast/nuclear genome ratio was calculated relative to the appropriate control collected at the same time. The apicoplast/nuclear genome ratio was measured by qPCR two times.

Immunoblotting. Syringe-lysed parasites (1 ml of culture, representing one-fourth of the total sample) were washed with PBS and frozen in 1 \times NuPAGE LDS sample buffer (Invitrogen) prior to analysis. Proteins were separated by electrophoresis on a 4% to 12% Bis-Tris gel (Invitrogen) and transferred to a nitrocellulose membrane. After blocking, membranes were probed with a 1:5,000 dilution of polyclonal rabbit anti-*TgCpn60* (gift from Boris Striepen, University of Pennsylvania) and a 1:10,000 dilution of IRDye 800RD donkey anti-rabbit antibody (LiCor Bioscience, Lincoln, NE). Fluorescence antibody-bound proteins were detected with an Odyssey imager (LiCor Biosciences). Immunoblot analyses were performed 2 times.

Statistical analysis. When applicable, data were analyzed using GraphPad Prism software and expressed as mean values \pm standard errors of the means (SEM). Basic experiments were repeated at least twice, including both positive and negative controls. Biological replicates were performed on different days or on independent cultures, while technical replicates were performed using cells from the same culture. Experiments were not blind. All new reagents were validated prior to use. All qPCR primers were assessed for single amplicons.

SUPPLEMENTAL MATERIAL

Supplemental material for this article may be found at <https://doi.org/10.1128/AAC.01646-18>

SUPPLEMENTAL FILE 1, PDF file, 0.4 MB.

ACKNOWLEDGMENTS

We thank Boris Striepen for providing *T. gondii* FNR-RFP and the *TgCpn60* antibody. We also thank Louis Weiss, Vincent Tu, and Joshua Mayoral for their support and assistance with drug assays.

This project has been funded with federal funds from the NIH under award numbers 1K08AI097239 (E.Y.), 1DP5OD012119 (E.Y.), and T32GM007276 (K.A.-J.). Funding was also provided by the Burroughs-Wellcome Fund (E.Y.), the Chan Zuckerberg Biohub (E.Y.), and the Stanford Bio-X SIGF William and Lynda Steere Fellowship (K.A.-J.). The funders had no role in study design, data collection and interpretation, or the decision to submit the work for publication.

REFERENCES

- Kohler S, Delwiche CF, Denny PW, Tilney LG, Webster P, Wilson RJ, Palmer JD, Roos DS. 1997. A plastid of probable green algal origin in apicomplexan parasites. *Science* 275:1485–1489. <https://doi.org/10.1126/science.275.5305.1485>.
- McFadden GI, Reith ME, Munholland J, Lang-Unnasch N. 1996. Plastid in human parasites. *Nature* 381:482. <https://doi.org/10.1038/381482a0>.
- Janouskovec J, Horak A, Obornik M, Lukes J, Keeling PJ. 2010. A common red algal origin of the apicomplexan, dinoflagellate, and heterokont

- plastids. *Proc Natl Acad Sci U S A* 107:10949–10954. <https://doi.org/10.1073/pnas.1003335107>.
4. Mazumdar J, Wilson EH, Masek K, Hunter CA, Striepen B. 2006. Apicoplast fatty acid synthesis is essential for organelle biogenesis and parasite survival in *Toxoplasma gondii*. *Proc Natl Acad Sci U S A* 103:13192–13197.
 5. Nair SC, Brooks CF, Goodman CD, Strum A, McFadden GI, Sundriyal S, Anglin JL, Song Y, Moreno SNJ, Striepen B. 2011. Apicoplast isoprenoid precursor synthesis and the molecular basis of fosmidomycin resistance in *Toxoplasma gondii*. *J Exp Med* 208:1547–1559. <https://doi.org/10.1084/jem.20110039>.
 6. Yeh E, DeRisi JL. 2011. Chemical rescue of malaria parasites lacking an apicoplast defines organelle function in blood-stage *Plasmodium falciparum*. *PLoS Biol* 9:e1001138. <https://doi.org/10.1371/journal.pbio.1001138>.
 7. Rolston KV. 1991. Treatment of acute toxoplasmosis with oral clindamycin. *Eur J Clin Microbiol Infect Dis* 10:181–183. <https://doi.org/10.1007/BF01964456>.
 8. Geary TG, Jensen JB. 1983. Effects of antibiotics on *Plasmodium falciparum* in vitro. *Am J Trop Med Hyg* 32:221–225. <https://doi.org/10.4269/ajtmh.1983.32.221>.
 9. Fichera ME, Bhopale MK, Roos DS. 1995. In vitro assays elucidate peculiar kinetics of clindamycin action against *Toxoplasma gondii*. *Antimicrob Agents Chemother* 39:1530–1537. <https://doi.org/10.1128/AAC.39.7.1530>.
 10. Fichera ME, Roos DS. 1997. A plastid organelle as a drug target in apicomplexan parasites. *Nature* 390:407–409. <https://doi.org/10.1038/37132>.
 11. Dahl EL, Shock JL, Shenai BR, Gut J, DeRisi JL, Rosenthal PJ. 2006. Tetracyclines specifically target the apicoplast of the malaria parasite *Plasmodium falciparum*. *Antimicrob Agents Chemother* 50:3124–3131. <https://doi.org/10.1128/AAC.00394-06>.
 12. Amberg-Johnson K, Hari SB, Ganesan SM, Lorenzi HA, Sauer RT, Niles JC, Yeh E. 2017. Small molecule inhibition of apicomplexan FtsH1 disrupts plastid biogenesis in human pathogens. *Elife* 6:e29865. <https://doi.org/10.7554/eLife.29865>.
 13. Camps M, Arrizabalaga G, Boothroyd J. 2002. An rRNA mutation identifies the apicoplast as the target for clindamycin in *Toxoplasma gondii*. *Mol Microbiol* 43:1309–1318. <https://doi.org/10.1046/j.1365-2958.2002.02825.x>.
 14. Ralph SA, van Dooren GG, Waller RF, Crawford MJ, Fraunholz MJ, Foth BJ, Tonkin CJ, Roos DS, McFadden GI. 2004. Tropical infectious diseases: metabolic maps and functions of the *Plasmodium falciparum* apicoplast. *Nat Rev Microbiol* 2:203–216. <https://doi.org/10.1038/nrmicro843>.
 15. Martins-Duarte ES, Carias M, Vommaro R, Surolia N, de Souza W. 2016. Apicoplast fatty acid synthesis is essential for pellicle formation at the end of cytokinesis in *Toxoplasma gondii*. *J Cell Sci* 129:3320–3331. <https://doi.org/10.1242/jcs.185223>.
 16. McLeod R, Muench SP, Rafferty JB, Kyle DE, Mui EJ, Kirisits MJ, Mack DG, Roberts CW, Samuel BU, Lyons RE, Dorris M, Milhous WK, Rice DW. 2001. Triclosan inhibits the growth of *Plasmodium falciparum* and *Toxoplasma gondii* by inhibition of apicomplexan Fab I. *Int J Parasitol* 31:109–113. [https://doi.org/10.1016/S0020-7519\(01\)00111-4](https://doi.org/10.1016/S0020-7519(01)00111-4).
 17. Reiff SB, Vaishnav S, Striepen B. 2012. The HU protein is important for apicoplast genome maintenance and inheritance in *Toxoplasma gondii*. *Eukaryot Cell* 11:905–915. <https://doi.org/10.1128/EC.00029-12>.
 18. Frenal K, Jacot D, Hammoudi PM, Graindorge A, Maco B, Soldati-Favre D. 2017. Myosin-dependent cell-cell communication controls synchronicity of division in acute and chronic stages of *Toxoplasma gondii*. *Nat Commun* 8:15710. <https://doi.org/10.1038/ncomms15710>.
 19. Crawford MJ, Thomsen-Zieger N, Ray M, Schachtner J, Roos DS, Seeber F. 2006. *Toxoplasma gondii* scavenges host-derived lipoic acid despite its de novo synthesis in the apicoplast. *EMBO J* 25:3214–3222. <https://doi.org/10.1038/sj.emboj.7601189>.
 20. Agrawal S, Chung DW, Ponts N, van Dooren GG, Prudhomme J, Brooks CF, Rodrigues EM, Tan JC, Ferdig MT, Striepen B, Le Roch KG. 2013. An apicoplast localized ubiquitylation system is required for the import of nuclear-encoded plastid proteins. *PLoS Pathog* 9:e1003426. <https://doi.org/10.1371/journal.ppat.1003426>.
 21. Sheiner L, Fellows JD, Ovcariakova J, Brooks CF, Agrawal S, Holmes ZC, Bietz I, Flinner N, Heiny S, Mirus O, Przyborski JM, Striepen B. 2015. *Toxoplasma gondii* Toc75 functions in import of stromal but not peripheral apicoplast proteins. *Traffic* 16:1254–1269. <https://doi.org/10.1111/tra.12333>.
 22. van Dooren GG, Reiff SB, Tomova C, Meissner M, Humbel BM, Striepen B. 2009. A novel dynamin-related protein has been recruited for apicoplast fission in *Toxoplasma gondii*. *Curr Biol* 19:267–276. <https://doi.org/10.1016/j.cub.2008.12.048>.
 23. van Dooren GG, Tomova C, Agrawal S, Humbel BM, Striepen B. 2008. *Toxoplasma gondii* Tic20 is essential for apicoplast protein import. *Proc Natl Acad Sci U S A* 105:13574–13579. <https://doi.org/10.1073/pnas.0803862105>.
 24. Black MW, Boothroyd JC. 2000. Lytic cycle of *Toxoplasma gondii*. *Microbiol Mol Biol Rev* 64:607–623. <https://doi.org/10.1128/MMBR.64.3.607-623.2000>.
 25. Striepen B, Crawford MJ, Shaw MK, Tilney LG, Seeber F, Roos DS. 2000. The plastid of *Toxoplasma gondii* is divided by association with centrosomes. *J Cell Biol* 151:1423–1434. <https://doi.org/10.1083/jcb.151.7.1423>.
 26. Agrawal S, van Dooren GG, Beatty WL, Striepen B. 2009. Genetic evidence that an endosymbiont-derived endoplasmic reticulum-associated protein degradation (ERAD) system functions in import of apicoplast proteins. *J Biol Chem* 284:33683–33691. <https://doi.org/10.1074/jbc.M109.044024>.
 27. Li ZH, Ramakrishnan S, Striepen B, Moreno SN. 2013. *Toxoplasma gondii* relies on both host and parasite isoprenoids and can be rendered sensitive to atorvastatin. *PLoS Pathog* 9:e1003665. <https://doi.org/10.1371/journal.ppat.1003665>.
 28. Lim L, McFadden GI. 2010. The evolution, metabolism and functions of the apicoplast. *Philos Trans R Soc Lond B Biol Sci* 365:749–763. <https://doi.org/10.1098/rstb.2009.0273>.
 29. Bisanz C, Bastien O, Grand D, Jouhet J, Marechal E, Cesbron-Delauw MF. 2006. *Toxoplasma gondii* acyl-lipid metabolism: de novo synthesis from apicoplast-generated fatty acids versus scavenging of host cell precursors. *Biochem J* 394:197–205. <https://doi.org/10.1042/BJ20050609>.
 30. Coppens I. 2006. Contribution of host lipids to *Toxoplasma* pathogenesis. *Cell Microbiol* 8:1–9. <https://doi.org/10.1111/j.1462-5822.2005.00647.x>.
 31. Hu X, Binns D, Reese ML. 2017. The coccidian parasites *Toxoplasma* and *Neospora* dysregulate mammalian lipid droplet biogenesis. *J Biol Chem* 292:11009–11020. <https://doi.org/10.1074/jbc.M116.768176>.
 32. Dahl EL, Rosenthal PJ. 2007. Multiple antibiotics exert delayed effects against the *Plasmodium falciparum* apicoplast. *Antimicrob Agents Chemother* 51:3485–3490. <https://doi.org/10.1128/AAC.00527-07>.
 33. Lamarque MH, Roques M, Kong-Hap M, Tonkin ML, Rugarabamu G, Marq JB, Penarete-Vargas DM, Boulanger MJ, Soldati-Favre D, Lebrun M. 2014. Plasticity and redundancy among AMA-RON pairs ensure host cell entry of *Toxoplasma* parasites. *Nat Commun* 5:4098. <https://doi.org/10.1038/ncomms5098>.
 34. Pfaffl MW. 2001. A new mathematical model for relative quantification in real-time RT-PCR. *Nucleic Acids Res* 29:e45. <https://doi.org/10.1093/nar/29.9.e45>.